PCCP

Accepted Manuscript

ROYAL SOCIETY OF CHEMISTRY

www.rsc.org/pccp

PCCP

ARTICLE

Relationship between Low-*Q* Peak and Long-range Ordering of Ionic Liquids Revealed by High-Energy X-ray Total Scattering

Received 00th January 20xx,
Accepted 00th January 20xx

DOI: 10.1039/x0xx00000x

www.rsc.org/

Kenta Fujii,*[a] Shinji Kohara,[b] and Yasuhiro Umebayashi*[c]

The structures of 1-alkyl-3-methylimidazolium bis(trifluoromethanesulfonyl)amide ([C_nmIm$^+$][TFSA$^-$]) ionic liquids (alkyl-chain length n = 4, 8, 10, and 12) have been studied by high-energy X-ray total scattering at T = 298–453 K. The low-Q peaks observed in the X-ray structure factors $S(Q)$s at 0.2 < Q < 0.4 Å^{-1} for $n \leq 8$ were almost unchanged up to T = 453 K, whereas they shifted to lower Q value and peak intensity decreased for n = 10 and 12. The radial distribution functions $G(r)$s for $n \leq 8$ showed no temperature dependence, but the $G(r)$s in the long r region showed significant temperature dependence, especially for r = 15–25 Å for n = 10 and 12. To discuss the relationship between the low-Q peak intensity in $S(Q)$ and the profile of $G(r)$ at long range, we propose a new function $S^{Qpeak}(r)$. It is elucidated that the low-Q peak observed for n = 12 is a signature of long-range ordering in the r range 15–25 Å, which corresponds to both of the anion–anion correlations at the first neighbor and the alkyl group aggregates among the C_{12}mIm$^+$ cations, whereas the anion–anion correlations at the first neighbor are predominant for reproducing the low-Q peaks in the n = 8 and 10 systems.

Introduction

Room temperature ionic liquids (ILs) consist only of ions, and thus their solvent properties differ greatly and essentially from those of neutral molecular solvents such as water and conventional organic solvents. ILs, therefore, show unique properties such as nonvolatility, nonflammability, high ionic conductivity, and, in particular, high designability by adjusting their constituent ions.[1-3] The designability of ILs allows us to control their solvent properties arising from intermolecular interactions between the ions. By changing the molecular structure of the ions and/or the combination of cations and anions, we can easily and selectively add specific interactions such as hydrogen bonding, hydrophobic, cation–π, and π–π interactions to IL solvents.[4-7] Thus, numerous thermodynamic and structural studies on such intermolecular interactions have been conducted on several IL systems.

It is suggested by computer simulations and experiments that ILs with an alkyl group of long or intermediate chain length show nanoscale segregation. For ILs with alkyl-chain length n > 4, nanoscale segregation originates from the formation of nonpolar (alkyl-chain aggregates) and polar (the charged moieties of the cation and anion) domains.[5, 6, 8-12] Small-angle X-ray and neutron scattering (SAXS and SANS, respectively) measurements are powerful tools to observe the nanosegregation of ILs. Triolo et al. first reported that a characteristic peak is observed in imidazolium-based ILs with n > 4 in the low-Q region of 0.2–0.5 Å^{-1} (referred to as the "low-Q peak") by SAXS measurements.[13] Yamamuro et al. indicated the IL domains in terms of slow dynamics from ns to ps timescales by a neutron spin-echo technique.[14] They ascribed the low-Q peak in SAXS and SANS data to the formation of spherical nanoscale domains such as micelles or lamellae by aggregation of the alkyl groups. The "low-Q peak" was also observed in ethylammonium and propylammonium nitrate (EAN and PAN, respectively) with short alkyl groups.[15, 16] Atkin et al. reported that the cation and anion in EAN and PAN significantly aggregate with each other to form nanoscale structures.[15] However, it might be expected that EAN and PAN are unable to form micelle-like structures due to their short alkyl chain lengths, n = 2 and 3, respectively. As an alternative interpretation for the low-Q peak, Margulis et al. proposed that it mainly originates from a characteristic distance between polar groups separated by long alkyl chains.[17-19] A similar interpretation was suggested on the basis of coarse-grained and all-atom molecular dynamics (MD) simulations by Balasubramanian et al.,[20-22] who proposed a strong relationship between the low-Q peak and spatial distance between the anions. Furthermore, Hardacre et al. performed SANS measurements in combination with an H/D isotopic substitution technique on typical imidazolium-based ILs and found that the spatial distance between the charged imidazolium rings at the second coordination shell separated by the alkyl groups was important in understanding the origin of the low-Q peak.[23] From a thermodynamic perspective, the n dependence of vaporization enthalpy, $\Delta_{vap}H$ (or cohesive

[a] Graduate School of Science and Engineering, Yamaguchi University, 2-16-1 Tokiwadai, Ube, Yamaguchi 755-8611, Japan. E-mail: k-fujii@yamaguchi-u.ac.jp
[b] Japan Synchrotron Radiation Research Institute (JASRI), Sayo-cho, Sayo-gun, Hyogo 679-5198, Japan.
[c] Graduate School of Science and Technology Niigata University, 8050 Ikarashi, 2-no-cho, Nishi-ku, Niigata 950-2181, Japan.
† Electronic Supplementary Information (ESI) available: Experimental S(Q)s (Q-range: 0-25 Å). See DOI: 10.1039/x0xx00000x

energy), for 1-alkyl-3-methylimidazolium (C_nmIm$^+$)-based ILs with n = 2–8 was calculated by MD simulations.[24, 25] It was found that $\Delta_{vap}H$ increases with increasing n, and this was quantitatively discussed by decomposing the total $\Delta_{vap}H$ into Coulomb and van der Waals (VDW) contributions. The VDW component in $\Delta_{vap}H$ increases monotonically with increasing n, whereas the Coulomb component remains almost unchanged. This indicates that the alkyl groups of the C_nmIm$^+$ cation aggregate to enhance the nanosegregation in the ILs, and the polar domains remain unchanged in the interactions. We also investigated the origin of the low-Q peak for typical aprotic and protic ILs by high-energy X-ray total scattering (HEXTS), SANS, and MD simulations.[4, 26] We indicated that the intensity of the low-Q peak strongly depends on the structure at a real-space distance of 10–25 Å, which can be clearly shown by applying a newly introduced $S^{Q\text{peak}}(r)$ function. To obtain more detailed insight into the origin of the low-Q peak, HEXTS experiments have now been performed on 1-alkyl-3-methylimidazolium bis(trifluoromethanesulfonyl)amide ILs, [C_nmIm$^+$][TFSA$^-$] with n = 4–12, to reveal their structures at room temperature to high temperature.

Experimental

Materials.

[C_nmIm$^+$][TFSA$^-$] ILs were prepared by the standard method using 1-alkyl-3-methylimidazolium bromide ([C_nmIm$^+$][Br$^-$]) and HTFSA.[26, 27] The ILs thus obtained were dried in a vacuum desiccator over P_2O_5, and their water contents were less than 100 ppm according to the Karl–Fischer method.

High-energy X-ray total scattering (HEXTS) measurements.

HEXTS measurements were performed using a two-axis diffractometer built at BL04B2 beamline of SPring-8.[28, 29] Monochromated X-rays of energy 61.6 keV were obtained using an Si (220) monochromator. The sample in a quartz capillary was placed in an electrical furnace, and the temperature was raised from 298 to 453 K. The observed X-ray intensity was corrected for absorption,[30] polarization, and incoherent scatterings[31, 32] to obtain the coherent scattering intensity, $I_{coh}(Q)$.

The X-ray structure factor $S(Q)$ and radial distribution function $G(r)$ per stoichiometric volume containing a [C_nmIm$^+$][TFSA$^-$] ion-pair were obtained according to

$$S(Q)=\frac{I_{coh}(Q)-\sum n_i f_i^2(Q)}{(\sum n_i f_i(Q))^2}+1 \quad (1)$$

and

$$G(r)-1=\frac{1}{2\pi^2 r\rho_0}\int_0^Q Q[S(Q)-1]\sin(Qr)\exp(-BQ^2)dQ, \quad (2)$$

respectively, where n_i and $f_i(Q)$ denote the number and the atomic scattering factor of atom i, respectively, ρ_0 is the number density, and B is the damping factor (0.008 or 0.1 Å^2 in this study).

Results and discussion

HEXTS.

Figure 1 shows structure factors $S(Q)$s in the Q-range of 0–2.5 Å^{-1} for [C_nmIm$^+$][TFSA$^-$] with n = 4, 8, 10, and 12 obtained from HEXTS measurements at 298, 376, and 453 K. The corresponding $S(Q)$s over the entire Q-range (0–20.0 Å^{-1}) are shown in Figure S1. In the Q-range 0.4–2.0 Å^{-1}, the T dependence of $S(Q)$ was seen to be similar among all the [C_nmIm$^+$][TFSA$^-$]s. The peak at around Q = 1.4 Å^{-1} gradually shifted to the lower-Q side, and the peak at around Q = 0.8 Å^{-1} was intensified with increasing T. This behavior indicated that there was almost no change in the short-range intermolecular interactions, such as nearest-neighbor cation–anion interaction, even with varying T. Conversely, in $S(Q)$ at Q < 0.4 Å^{-1} (hereinafter, the "low-Q peak"), the variation with changing T was seen to depend on the alkyl-chain length n. The intensity of the low-Q peak for n = 8 was unchanged even with increasing T. The intensity for n = 10 was slightly weakened with increasing T up to 376 K, but thereafter remained unchanged with a further increase in T. In the case of n = 12, the intensity of the low-Q peak significantly decreased with increasing T, and the peak position of Q = 0.2 Å^{-1} shifted toward higher Q to reach Q = 0.3 Å^{-1} at 453 K. Figure 2 shows radial distribution functions in the form $r^2[G(r) - 1]$ in the r range below 15 Å for n = 4, 8, 10, and 12 with varying T. Almost no change in $r^2[G(r) - 1]$ was observed for the n = 4 and 8 systems with varying T, which is consistent with the variation of the corresponding $S(Q)$. According to our previous study, it is noted that $G(r)$ in the r range up to 15 Å is

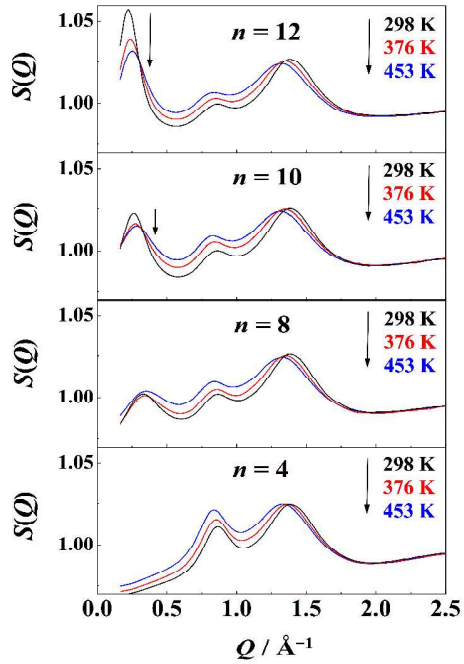

Fig. 1. Temperature dependences of $S(Q)$s for [C_nmIm$^+$][TFSA$^-$]s with alkyl-chain lengths n = 4, 8, 10, and 12.

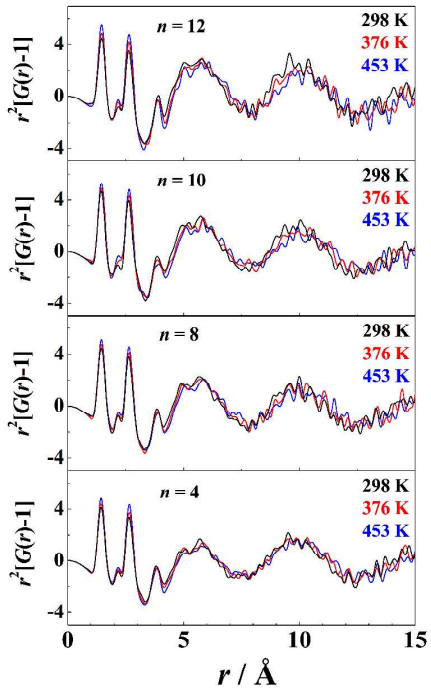

Fig. 2. Temperature dependences of $r^2[G(r) - 1]$ functions obtained for $[C_n mIm^+][TFSA^-]$s with n = 4, 8, 10, and 12 (B = 0.008).

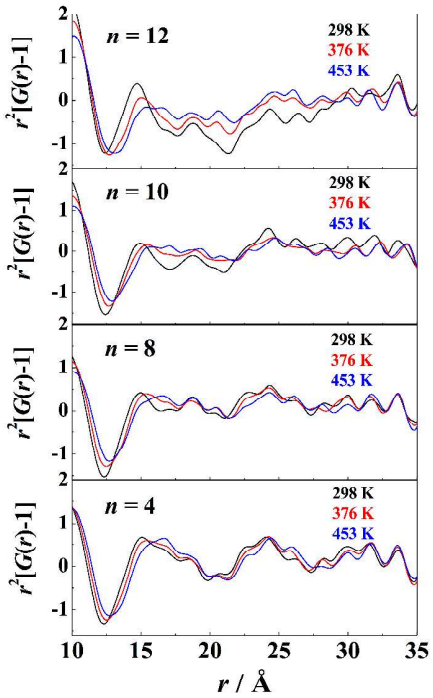

Fig. 3. Temperature dependences of $r^2[G(r) - 1]$ functions obtained for $[C_n mIm^+][TFSA^-]$s with n = 4, 8, 10, and 12 (B = 0.1).

mainly contributed by the closest ion–ion interactions, i.e., the first neighbors for the cation–anion and similar charged ion–ion interactions.[26] Therefore, the results suggest that the short-range structure of the ion–ion interactions remains unchanged in the ILs, irrespective of T. The same interpretation can be applied to $r^2[G(r) - 1]$ for n = 10 and 12 at r < 8 Å, suggesting no T dependence of the closest ion–ion interactions. However, it seems that the amplitude in $r^2[G(r) - 1]$ above 8 Å slightly depends on T. To discuss the variation in the long r range in detail, we calculated $r^2[G(r) - 1]$ over the r range up to 35 Å using a large damping factor B = 0.1, as shown in Figure 3. The $r^2[G(r) - 1]$ functions for n = 4 and 8 are almost the same at each T. It is thus expected that the long-range ordering in both ILs is not disrupted even at high T. Conversely, for n = 10, the amplitude in $r^2[G(r) - 1]$ at r = 15–25 Å, showing a negative value at 298 K, obviously disappeared with increasing T to give no amplitude in this r range at 376 and 453 K. The trend was more clearly seen in the n = 12 system. The $r^2[G(r) - 1]$ function for the n = 12 system exhibits a valley centered at around 20 Å, which becomes shallow (or near to $r^2[G(r) - 1] = 0$) with increasing T. It is plausible that the valley, i.e., negative $r^2[G(r) - 1]$ (<0) in this r region, originates from alkyl group aggregation (dodecyl group) since the negative value of $r^2[G(r) - 1]$ means that the partial density at a given r is lower than the averaged density ($r^2[G(r) - 1] = 0$) in the solution. That is, the partial density of the alkyl group is lower than the average density of the $[C_{12}mIm^+][TFSA^-]$ including the ionic moieties. We thus conclude here that the aggregates of the alkyl groups are ruptured with increasing T to approach $r^2[G(r) - 1] \approx 0$.

Paschek et al. reported a systematic study on the T and n dependences of the vaporization enthalpy, $\Delta_{vap}H$ (or cohesive energy), for $[C_n mIm^+][TFSA^-]$ systems calculated by MD simulations.[24] In the T dependence, $\Delta_{vap}H$ was seen to decrease linearly with increasing T, which was discussed in detail by decomposing the total $\Delta_{vap}H$ into the respective contributions from Coulomb and van der Waals (VDW) interactions. The VDW component in $\Delta_{vap}H$ for ILs with long alkyl groups showed a larger T dependence than the Coulomb component, i.e., the decrease in the total $\Delta_{vap}H$ could be almost entirely attributed to that in the VDW component, whereas there was no significant contribution from the Coulomb term. The results of theoretical studies from a thermodynamic perspective are consistent with our experimental data. Here, we note that the low-Q peak stems mainly from two components for the long-range structures, i.e., the alkyl-chain aggregate (VDW) and the charge component (Coulomb). To reveal their long-range structure effects on the low-Q peak intensity, we introduce a new function $S^{Qpeak}(r)$.

$S^{Qpeak}(r)$ function; relationship between low-Q peak and real space structure.

As reported in our previous studies,[4, 26] $S^{Qpeak}(r)$ functions are useful to understand the relationship between a low-Q peak intensity in $S(Q)$ and a real r-space structure in $G(r)$. According to a simple definition rationalized by the mutual Fourier transform between $S(Q)$ and $G(r)$, $S^{Qpeak}(r)$ can be easily calculated by integrating the experimental $r^2[G(r) - 1]$ multiplied by $\sin(Qr)/Qr$ up to r_{max} as follows:

$$S^{Q_{peak}}(r) = 4\pi\rho_0 \int_0^{r_{max}} r^2 [G(r)-1] \frac{\sin(Qr)}{Qr} dr + 1 \quad (3)$$

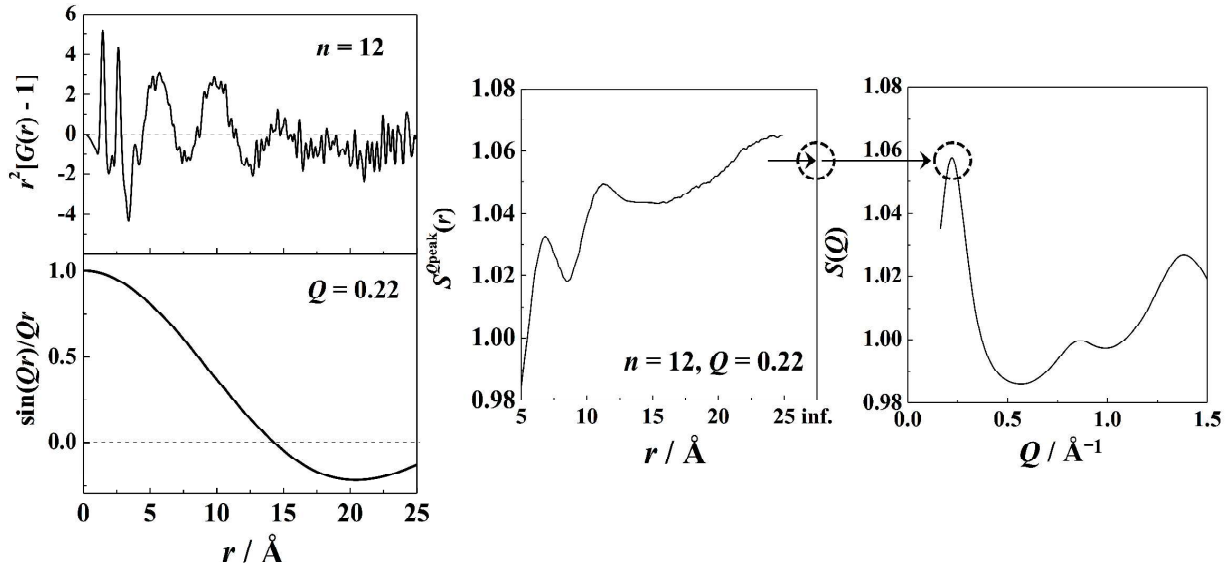

Fig. 4. (a) Experimental $r^2[G(r) - 1]$ for n = 12 (T = 298 K), (b) $\sin(Qr)/Qr$ at Q = 0.22 Å, (c) $S^{Qpeak}(r)$ calculated by Equation (3), and (d) experimental $S(Q)$.

When Q is given as a peak position Q_{peak} of the observed low-Q peak, we can evaluate $S^{Qpeak}(r)$ over a variable integration range up to r_{max} (in this study, r_{max} = 25 Å). Figure 4 (a) and (b) show the experimental $r^2[G(r) - 1]$ for $[C_{12}mIm^+][TFSA^-]$ at 298 K and the $\sin(Qr)/Qr$ function with Q = 0.22 $Å^{-1}$ corresponding to the Q_{peak}, respectively. The $S^{Qpeak}(r)$ was thus evaluated as a function of r based on the two functions in Figure 4 (a) and (b), and is shown in Figure 4 (c). If r is increased up to an infinite value (r_{max} = ∞), $S^{Qpeak}(r)$ approaches the low-Q peak intensity indicated by the arrow in Figure 4 (d). The r_{max} = 25 Å in this study yielded an $S^{Qpeak}(r)$ value of 1.07, which is comparable to the low Q-peak intensity (1.06). As can be seen in Figure 4 (c), $S^{Qpeak}(r)$ showed the intensity increase in three r regions of (I) 5–8 Å, (II) 10–12 Å, and (III) > 18 Å, suggesting that the liquid structures in these r regions made the main contributions to the low-Q peak intensity. In previous studies,[26, 33, 34] we have already reported the results of X-ray experiments and MD simulations, which showed that the liquid structures in regions (I), (II), and (III) correspond to the closest cation–anion interactions, the similar charged ion–ion correlations (particularly the anion–anion correlation), and alkyl-chain aggregations among cations, respectively.

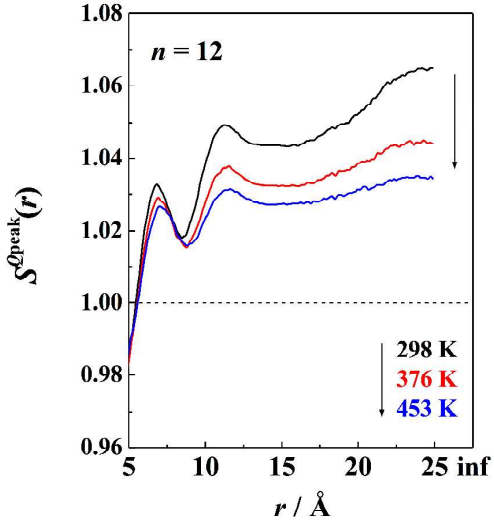

Fig. 5. Temperature dependence of $S^{Qpeak}(r)$ for $[C_{12}mIm^+][TFSA^-]$.

Figure 5 shows the T dependence of $S^{Qpeak}(r)$ observed for $[C_{12}mIm^+][TFSA^-]$. A significant T dependence was observed in the r regions (II) and (III), whereas it was not significant in r region (I). In region (I), as mentioned above, the increase in the $S^{Qpeak}(r)$ intensity from r = 5 to 8 Å mainly corresponds to the closest cation–anion interactions in real space. According to the theoretical $\Delta_{vap}H$ obtained by MD simulations,[24] the Coulomb contribution to the total $\Delta_{vap}H$ is almost independent of T. It is thus expected that the cation–anion interactions at the first neighbor hardly depend on T and then the averaged structure remains unchanged even at higher T. In fact, the short r range correlations ($r^2[G(r) - 1]$ in Figure 2) were almost the same even at the T values examined here leading to a similar variation in $S^{Qpeak}(r)$ in the region (I). We can thus conclude that the short-range structures at around r < 8 Å do not contribute to the T dependence of the low-Q peak intensity. In the r region (II), which mainly corresponds to the anion–anion correlations, the extent of the increase in the $S^{Qpeak}(r)$ becomes small with increasing T. This behavior suggests that the anion–anion correlations at the first neighbor around 10–12 Å are weakened with increasing T, resulting in a decrease in the low-Q peak intensity. In the r region (III) above 18 Å, $S^{Qpeak}(r)$ showed a marked decrease in

intensity with increasing *T*. The extent of this intensity decrease was larger than that in the *r* region (II). As mentioned above, $S^{Qpeak}(r)$ in region (III) is mainly ascribed to the alkyl-chain aggregates of the cations. It is thus plausible that these aggregates of the alkyl groups are ruptured with increasing *T* to give the significant decrease in $S^{Qpeak}(r)$ in region (III). This result is in good agreement with that from thermodynamic considerations,[24, 25] that is, the VDW component (alkyl-group aggregates) of the total cohesive energy decreases with increasing *T*, whereas the Coulomb component is almost independent of *T*. We thus conclude that the intense low-*Q* peak observed for the *n* = 12 system originates mainly from the alkyl-group aggregates of the $C_{12}mIm^+$ cations.

Figure 6 shows $S^{Qpeak}(r)$ obtained for the *n* = 10 system with varying *T*. There was essentially no *T* dependence of the $S^{Qpeak}(r)$, which was also the case for the *n* = 8 system.

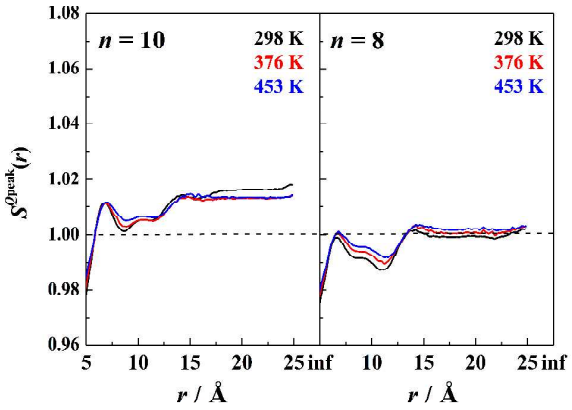

Fig. 6. Temperature dependences of $S^{Qpeak}(r)$s for $[C_{10}mIm^+][TFSA^-]$ and $[C_8mIm^+][TFSA^-]$. The *Q* values are 0.30 and 0.34 $Å^{-1}$, respectively.

However, a slight difference was seen above 15 Å between 298 K and the other temperatures. The $S^{Qpeak}(r)$ at $r > 15$ Å decreased in intensity with an increase in *T* from 298 to 376 K, and thereafter showed no further change with increasing *T*. This slight decrease can be attributed to the rupture of the aggregates of the decyl groups of the $C_{10}mIm^+$ cations as for the *n* = 12 system described above. The magnitude of the VDW interactions among the decyl groups is less than that among the dodecyl groups, resulting in a smaller *T* dependence of $S^{Qpeak}(r)$ at $r < 15$ Å, or the low-*Q* peak intensity, for *n* = 10 than for *n* = 12.

Conclusions

HEXTS experiments at varying *T* have been performed on $[C_nmIm^+][TFSA^-]$ ILs to obtain their *S*(*Q*)s and *G*(*r*)s. It was found that the intensity variation of the low-*Q* peak versus *T* (298–453 K) showed a strong dependence on the alkyl-chain length *n* of the C_nmIm^+ cations. That is to say, the low-*Q* peak intensity for *n* = 12 is significantly weakened with increasing *T*, whereas those for $n \leq 10$ remain unchanged. To directly connect the low-*Q* peak intensity with the real-space structure, we have introduced the $S^{Qpeak}(r)$ function to rationalize the observed X-ray data. On the basis of $S^{Qpeak}(r)$, we conclude that structures at the three *r* regions (I) 5–8 Å, (II) 10–12 Å, and (III) above 18 Å are important for the appearance of the low-*Q* peak in these $[C_nmIm^+][TFSA^-]$ systems. For the *n* = 12 system, which showed a significant low-*Q* peak, the structures in regions (II) and (III) were predominant, which correspond to anion–anion correlations at the first neighbor and the alkyl group aggregates among the $C_{12}mIm^+$ cations, respectively. The alkyl group aggregates in the *n* = 12 system were ruptured with increasing *T*, resulting in a decrease in the low-*Q* peak intensity. In the *n* = 8 and 10 systems, the low-*Q* peak intensity stemmed mainly from the correlations between the anions with no contribution from the alkyl-group aggregates. Consequently, the low-*Q* peak intensity was independent of *T*, which was supported by thermodynamic results (cohesive energies for ILs) obtained by MD simulations.

Acknowledgments

This study has been financially supported by Grants-in-Aid of Scientific Research from the Ministry of Education, Culture, Sports, Science and Technology (Nos. 24750066 to K.F., 24655142 to Y.U.), and the Advanced Low Carbon Technology Research and Development Program (ALCA) of the Japan Science and Technology Agency (JST). The HEXTS experiment was performed at BL04B2 of SPring-8 with the approval of the Japan Synchrotron Radiation Research Institute (JASRI) (Proposal nos. 2012B1502, 2012B1709, and 2013B1375).

Notes and references

1. P. Wasserscheid and T. Welton, Eds., *Ionic Liquids in Synthesis, Second Edition*, VCH-Wiley, Weinheim, 2008.
2. T. Welton, *Chem. Rev.*, 1999, 99, 2071-2083.
3. M. Armand, F. Endres, D. R. MacFarlane, H. Ohno and B. Scrosati, *Nat. Mater.*, 2009, 8, 621-629.
4. X. Song, H. Hamano, B. Minofar, R. Kanzaki, K. Fujii, Y. Kameda, S. Kohara, M. Watanabe, S. Ishiguro and Y. Umebayashi, *J. Phys. Chem. B*, 2012, 116, 2801-2813.
5. J. N. A. C. Lopes and A. A. H. Pádua, *J. Phys. Chem. B*, 2006, 110, 3330.
6. A. A. H. Pádua, M. F. C. Gomes and J. N. A. C. Lopes, *Acc. Chem. Res.* , 2007, 40, 1087.
7. K. Shimizu, M. F. C. Gomes, A. A. H. Pádua, L. P. N. Rebelo and J. N. A. C. Lopes, *J. Phys. Chem. B*, 2009, 113, 9894.
8. J. N. A. C. Lopes, M. F. C. Gomes and A. A. H. Pádua, *J. Phys. Chem. B* 2006, 110, 16816.
9. A. Triolo, O. Russina, H.-J. Bluif and E. D. Cola, *J. Phys. Chem. B*, 2007, 111, 4641-4644.
10. A. Triolo, O. Russina, B. Fazio, R. Triolo and E. D. Cola, *Chem. Phys. Lett.*, 2008, 457, 362–365.
11. H. K. Kashyap, C. S. Santos, R. P. Daly, J. J. Hettige, N. S. Murthy, H. Shirota, E. W. Castner Jr and C. J. Margulis, *J. Phys. Chem. B*, 2013, 117, 1130-1135.
12. H. K. Kashyap, C. S. Santos, N. S. Murthy, J. J. Hettige, K. Kerr, S. Ramati, J. Gwon, M. Gohdo, S. I. Lall-Ramnarine, J. F. Wishart, C. J. Margulis and E. W. Castner Jr., *J. Phys. Chem. B*, 2013, 117, 15328-15337.

13. A. Triolo, O. Russina, U. Keiderling and J. Kohlbrecher, *J. Phys. Chem. B*, 2006, 110, 1513.
14. M. Kofu, M. Nagao, T. Ueki, Y. Kitazawa, Y. Nakamura, S. Sawamura, M. Watanabe and O. Yamamuro, *J. Phys. Chem. B*, 2013, 117, 2773-2781.
15. R. Atkin and G. G. Warr, *J. Phys. Chem. B*, 2008, 112, 4164-4166.
16. R. Hayes, S. Imberti, G. G. Warr and R. Atkin, *Phys. Chem. Chem. Phys.*, 2011, 13, 3237–3247.
17. H. V. R. Annapureddy, H. K. Kashyap, P. M. De Biase and C. J. Margulis, *J. Phys. Chem. B*, 2010, 114, 16838–16846.
18. C. S. Santos, H. V. R. Annapureddy, N. S. Murthy, H. K. Kashyap, E. W. Castner Jr. and C. J. Margulis, *J. Chem. Phys.*, 2011, 134, 064501.
19. H. K. Kashyap, J. J. Hettige, H. V. R. Annapureddy and C. J. Margulis, *Chem. Comm.*, 2012, 48, 5103-5105.
20. B. L. Bhargava, R. Devane, M. L. Klein and S. Balasubramanian, *Soft Matter*, 2007, 3, 1395–1400.
21. B. L. Bhargava, M. L. Klein and S. Balasubramanian, *ChemPhysChem.*, 2008, 9, 67-70.
22. B. L. Bhargava, S. Balasubramanian and M. L. Klein, *Chem. Commun.*, 2008, 3339–3351.
23. C. Hardacre, J. D. Holbrey, C. L. Mullan, T. G. A. Youngs and D. T. Bowron, *J. Chem. Phys.*, 2010, 133, 074510.
24. T. Köddermann, D. Paschek and R. Ludwig, *ChemPhysChem.*, 2008, 9, 549 – 555.
25. L. M. N. B. F. Santos, J. N. A. C. Lopes, J. A. P. Coutinho, J. M. S. S. Esperança, L. R. Gomes, I. M. Marrucho and L. P. N. Rebelo, *J. Am. Chem. Soc.*, 2007, 129, 284-285.
26. K. Fujii, R. Kanzaki, T. Takamuku, Y. Kameda, S. Kohara, M. Kanakubo, M. Shibayama, S. Ishiguro and Y. Umebayashi, *J. Chem. Phys.*, 2011, 135, 244502.
27. K. Fujii, T. Nonaka, Y. Akimoto, Y. Umebayashi and S. Ishiguro, *Anal. Sci.*, 2008, 24, 1377-1380.
28. M. Isshiki, Y. Ohishi, S. Goto, K. Takeshita and T. Oshikawa, *Nucl. Instrum. Meth. A*, 2001, 467-468, 663.
29. S. Kohara, K. Suzuya, Y. Kashihara, N. Matsumoto, N. Umesaki and I. Sakai, *Nucl. Instrum. Meth. A*, 2001, 467-468, 1030.
30. S. Sakai, *KEK Report 90-16*, National Laboratory for High Energy Physics, Japan, 1990.
31. D. T. Cromer, *J. Chem. Phys.*, 1969, 50, 4857.
32. D. T. Cromer and R. J. Howerton, *J. Phys. Chem. Ref. Data*, 1975, 4, 471.
33. K. Fujii, Y. Soejima, Y. Kyoshoin, S. Fukuda, R. Kanzaki, Y. Umebayashi, T. Yamaguchi, S. Ishiguro and T. Takamuku, *J. Phys. Chem. B*, 2008, 112, 4329-4336.
34. K. Fujii, T. Mitsugi, T. Takamuku, T. Yamaguchi, Y. Umebayashi and S. Ishiguro, *Chem. Lett.*, 2009, 38, 340-341.

